Transition to chaos in a dissipative standardlike map

Sang-Yoon Kim and Duck-Sung Lee
Department of Physics, Kangwon National University, Chunchon, Kangwon-Do, 200-701, Korea
(Received 13 June 1991; revised manuscript received 13 November 1991)

We study the transition to chaos caused by overlap of resonances in a dissipative standardlike map exhibiting recurrence of invariant circles. In particular, the effects of the recurrence on the structure of a critical line at which the motion is always mode locked are investigated. When there is no recurrence of invariant circles, a smooth critical line exists. In the recurrence case, however, the critical line is folded back and has discontinuous parts. At this line the mode-locked intervals trace a folded devil's staircase with isolated parts. Scaling behavior of the complementary set to the folded staircase is also discussed.

PACS number(s): 05.45.+b, 03.20.+i, 05.70.Jk

I. INTRODUCTION

In recent years, much attention has been paid to the transition to chaos caused by overlap of resonances in dissipative dynamical systems that exhibit mode locking [1–13]. Mode locking is a resonant response occurring in systems with competing frequencies. In this paper we study dissipative systems with two competing frequencies. In the resonant region, the ratio of the two frequencies is rational. The onset of chaos is caused by overlap between the resonant regions, giving rise to hysteretic effects as well as chaotic behavior [7].

A model for this transition is the dissipative standard map [4,7]:

$$T:\begin{cases} r_{n+1}=br_n+k_g(\theta_n) \\ \theta_{n+1}=\theta_n+\Omega+r_{n+1}\ , \end{cases} \tag{1.1}$$

where $g(\theta)=g_s(\theta)=-(1/2\pi)\sin(2\pi\theta)$. This map has a constant Jacobian b, which serves as a dissipation parameter. For the area-preserving case, $b=1$, this is just the standard map [14,15], and in the singular limit, $b=0$, it reduces to the one-dimensional (1D) sine-circle map [3,6]. For the sine-circle map, the critical line, on which the measure of the mode-locked intervals is 1 and above which the smallest intervals start to overlap, is just $k=1$ [6], but no such simple relation exists generally for higher-dimensional systems. For the two-dimensional (2D) dissipative case ($0<b<1$), however, it has been found that a smooth critical line exists [7]. At this line the mode-locked intervals trace up a complete "devil's staircase." Universal scaling behavior of the complementary set to the staircase has also been studied.

Wilbrink [16] studied the conservative case ($b=1$) of a two-parameter standardlike map where the function g_s in Eq. (1.1) is replaced by

$$g_w(\theta)=-\frac{\sqrt{1+z}}{2\pi}\arcsin\left[\frac{\sin(2\pi\theta)}{\sqrt{1+z}}\right]. \tag{1.2}$$

He found that for small z values, invariant circles can reappear after their breakup. This is in contrast to the standard-map case [14,15] where there is no recurrence of invariant circles. Works on the quasiperiodic Schrödinger operator [17], the extended Frenkel-Kontorova model [18], and the extended standard map [19] also give similar results.

In this paper, we study the dissipative case ($0<b<1$) of the Wilbrink map (dissipative Wilbrink map) where the function g_s in Eq. (1.1) is replaced by g_w in Eq. (1.2). By varying the parameter z, the function $g_w(\theta)$ is tuned from a piecewise-linear function [16] ($z=0$) to the sine function $g_s(\theta)$ ($z=\infty$), and it is always analytic, except when $z=0$. Here we study the analytic case $z>0$.

In this dissipative Wilbrink map, one of us and Hu [13] studied the breakup of a specific invariant circle whose rotation number is the inverse golden mean, and found recurrence of the golden-mean invariant circle for small z values. There exists a critical dissipation-parameter value b_c, which is nonzero and depends on z. For $b\le b_c$ there is no recurrence of the golden-mean invariant circle, although "hourglass" structures exist in the nearby Arnol'd tongues. In this case the widths of the nearby tongues are not large enough for recurrence of the golden-mean invariant circle. However, as b is increased above b_c the nearby tongues become wider, and hence, near the thin parts of the hourglass the nearby resonances separate after they overlap near the thick parts. Therefore the golden-mean invariant circle in between them reappears near the thin parts after it has disappeared near the thick parts.

In this work, we study the global properties of the structure of mode locking, instead of concentrating on a specific irrational rotation number. In particular, we are interested in the effects of the recurrence of invariant circles on the structure of the critical line. For small z values it has been observed that, when dissipation is not strong, smooth invariant circles reappear after they have disappeared. In the recurrent region in (Ω,k) space, the critical line is folded back and has discontinuous parts. Thus it becomes a multivalued function of Ω with discontinuous parts. At this line the mode-locked intervals trace a folded devil's staircase with isolated parts. Scaling behavior of the complementary set to the folded staircase has also been studied.

This paper is organized as follows. In Sec. II the mode-locking structure and the method for constructing the critical line are discussed. In Sec. III we investigate the effects of the recurrence on the structure of the critical line. There, the scaling of the complement to the mode-locking set is also discussed. In Sec. IV a summary is given.

II. MODE LOCKING AND CRITICAL LINE

To study the mode locking in the dissipative Wilbrink map, we consider an orbit starting at $(\theta_0,r_0),(\theta_0,r_0),(\theta_1,r_1),\ldots$. An important quantity characterizing the orbit is the rotation number defined by

$$\omega=\lim_{n\to\infty}[(\theta_n-\theta_0)/n]\ . \tag{2.1}$$

The rotation number represents the average number of rotations per iteration.

Periodic orbits of period Q have rational rotation numbers P/Q if $\theta_Q=\theta_0+P$. The linear stability of a Q-cycle of rotation number P/Q is determined by the eigenvalues of the Jacobian matrix M which is the Q products of the linearized map along the orbit, where

$$M=\prod_{i=0}^{Q-1}\begin{bmatrix} b & kg'_w(\theta_i) \\ b & 1+kg'_w(\theta_i)\end{bmatrix}\ . \tag{2.2}$$

In the 2D dissipative case ($0<b<1$), the eigenvalues λ depend on both the trace (Tr) and the determinant (Det) of M:

$$\lambda=\tfrac{1}{2}\{\mathrm{Tr}M\pm[(\mathrm{Tr}M)^2-4\,\mathrm{Det}M]^{1/2}\}\ , \tag{2.3}$$

where $\mathrm{Det}M=b^Q$. If all the eigenvalues lie inside the unit circle, the orbit is stable. The linear stability is also determined in terms of a derived quantity, the residue [13,15], defined by

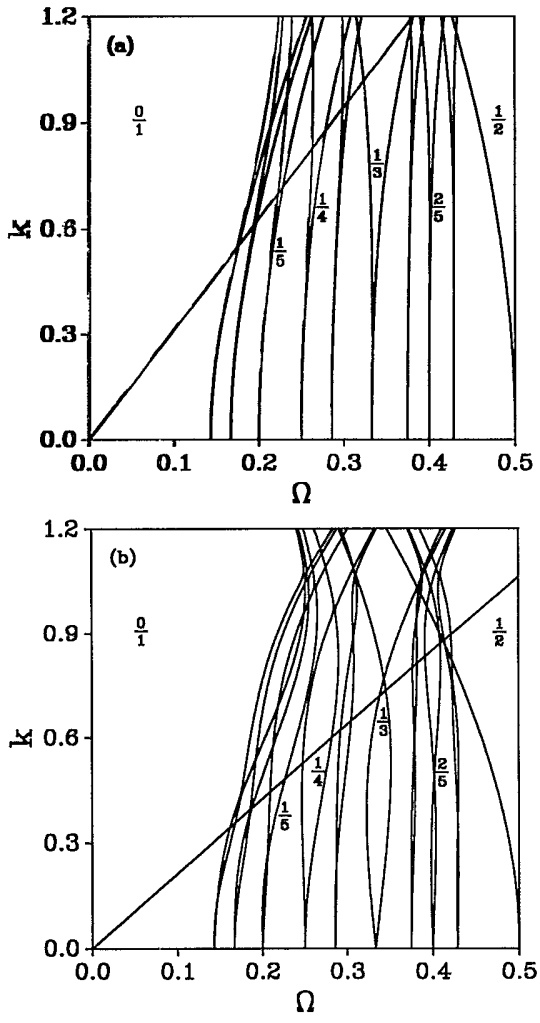

FIG. 1. Mode-locking diagrams for (a) the dissipative standard map with $b=0.5$ and for (b) the dissipative Wilbrink map with $z=0.01$ and $b=0.5$. The numbers are values of the rotation number ω.

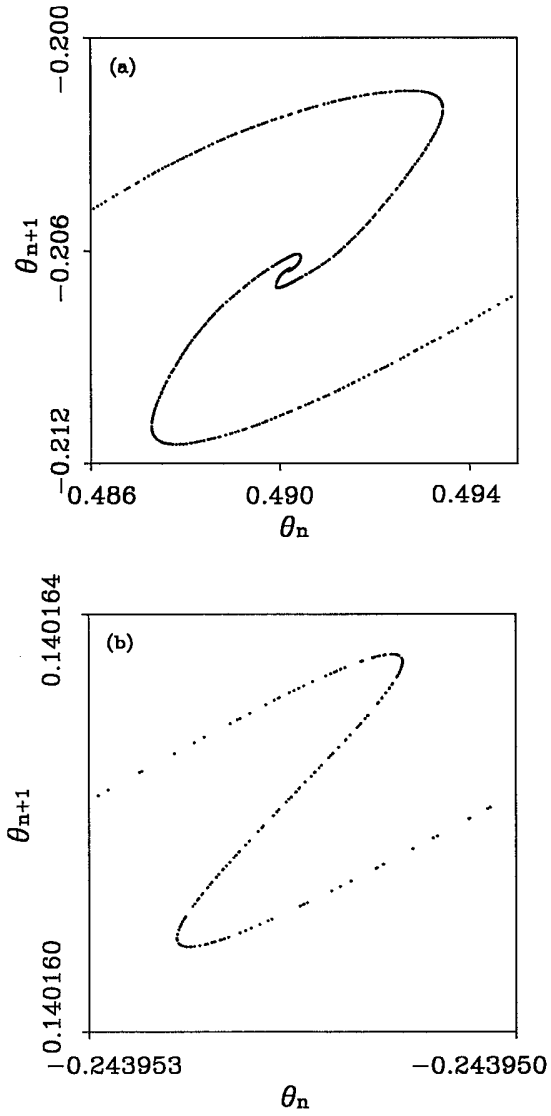

FIG. 2. Loss of smoothness of the invariant circle with $\omega=\frac{1}{3}$ shown by the reduced maps for the dissipative Wilbrink map with $z=0.01$ and $b=0.5$. (a) The curve spirals into a stable periodic point ($k=0.48$, $\Omega=0.338\,26$). (b) The curve crinkles up close to criticality ($k=0.3$, $\Omega=0.324$).

$$R=\frac{1+\mathrm{Det}M-\mathrm{Tr}M}{2(1+\mathrm{Det}M)} . \tag{2.4}$$

For a stable orbit, $0<R<1$; for an unstable orbit, $R<0$ or $R>1$.

The regime in (Ω,k) space where ω assumes a rational value P/Q is called the P/Q Arnol'd tongue. Inside the tongue the map has two Q-cycles of rotation number P/Q; one has a positive residue and the other a negative residue. The tongue boundary is determined by the condition

$$\lambda_{\max}=1 , \tag{2.5a}$$

where $\lambda_{\max}$ is the maximum eigenvalue, or

$$R=0 . \tag{2.5b}$$

Arnol'd tongues in the dissipative standard map are shown in Fig. 1(a). Note that the widths of all the tongues increase monotonically as k increases. In the dissipative Wilbrink map with small z values, however, "hourglass" structures exist in the P/Q Arnol'd tongues with $Q>2$ [see Fig. 1(b)]: The widths are not monotonically increasing functions of k. Narrowing of Arnol'd tongues has also been observed in certain circle maps [9,10] and commensurate-incommensurate phase transitions [20].

In the 1D case ($b=0$), no chaotic motion can occur for $k<1$, since there exist strong theorems [21] guaranteeing that any smooth, invertible, 1D map exhibits only periodic or quasiperiodic behavior. The critical line, on which the mode-locked intervals together occupy a set of full measure and above which the smallest tongues begin to overlap, is just $k=1$. Therefore no quasiperiodic orbits exist for $k>1$. However, for higher-dimensional maps, no simple criterion for the breakdown of smoothness of invariant circles exists.

In the 2D dissipative case ($0<b<1$), instead of looking at the original 2D map, we follow Bohr, Bak, and Jensen [7] by projecting out the angle variable θ and consider the 1D map $[\theta_{n+1}=f(\theta_n)]$, called a "reduced map." Just as for the circle-map case, the criterion for having smooth invariant circles is that the reduced map be smooth and invertible [7].

For a smooth invariant circle of rotation number P/Q, the attractor is a stable Q cycle. Associated with the stable Q cycle is an unstable Q cycle whose unstable manifold flows smoothly into the stable cycle and forms the invariant circle. In this case, the reduced map is smooth and invertible [7]. In general, there are two ways in which the invariant circle loses its smoothness: one is spiraling of the invariant circle and the other crinkling of it [2,5,7,11].

When the eigenvalues of M for the stable orbit are complex, the invariant circle spirals into each stable periodic point, and hence, at those points there is no unique direction of the tangent vector. Thus, the smoothness of the invariant circle is lost at the stable periodic points, which is shown by the reduced map in Fig. 2(a). Note that the monotonicity of the reduced map is lost. But, spiraling is not the only mechanism responsible for the loss of smoothness of the invariant circle. More generally, the invariant circle crinkles up and loses its smoothness at other parts except the stable periodic points; the direction of the tangent vector changes without limit as one approaches each stable periodic point. The crinkling of the invariant circle also produces the loss of monotonicity of the reduced map as shown in Fig. 2(b).

As an illustrative example, we consider the $\frac{1}{3}$ Arnol'd tongue and determine the critical line that separates the subcritical region, where a smooth invariant circle exists, and the supercritical one, where its smoothness is lost. Smoothness of an invariant circle of rotation number P/Q is lost at stable periodic points when the eigenvalues of M are complex. Therefore the stable periodic points become critical along a curve in (Ω,k) space where the eigenvalues are equal,

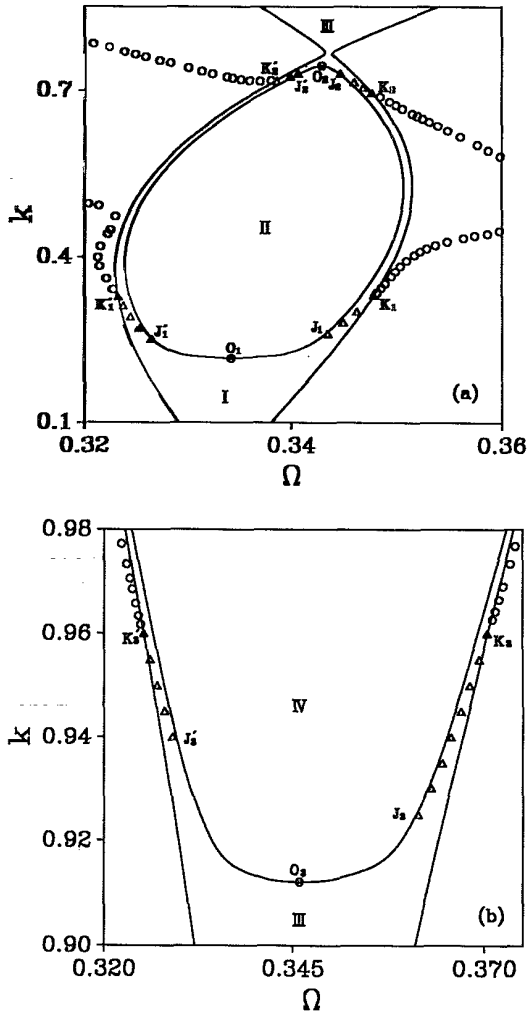

FIG. 3. Stability diagram for the invariant circles near the $\frac{1}{3}$ Arnol'd tongue in the dissipative Wilbrink map with $z=0.01$ and $b=0.5$. The representative points of the tongues are denoted by circles and the points at which crinkling up of invariant circles takes place by triangles. Inside the $\frac{1}{3}$ tongue, there are (a) an "ellipse" (2.6) and (b) a "hyperbola" (2.6). See text for other details.

$$\lambda_1=\lambda_2=\sqrt{\mathrm{Det}M}=b^{Q/2} \tag{2.6a}$$

or

$$R=\frac{(1-b^{Q/2})^2}{2(1+b^Q)} . \tag{2.6b}$$

For the $\frac{1}{3}$ Arnol'd tongue, there are two curves which satisfy the condition (2.6): one is a closed ellipse-shaped curve [see Fig. 3(a)] and the other an open hyperbola-shaped curve [see Fig 3(b)]. To locate the critical line, we must also know the more general crinkling up [Fig. 2(b)] takes place. This happens on curves connecting the curves (2.6) with the edges of the tongue. The triangles in Figs. 3(a) and 3(b) are points on these curves intersecting the curves (2.6) at J_i and J_i' and the tongue boundaries at K_i and K_i' $(i=1,2,3)$. Thus there exist three critical lines $K_iJ_iO_iJ_i'K_i'(i=1,2,3)$. Here $O_1(O_2)$ is the bottom (top) point on the "ellipse" with the smallest (largest) k and O_3 the bottom point on the "hyperbola" with the smallest k.

These critical lines divide the tongue into four regions denoted by I, II, III, and IV in Figs. 3(a) and 3(b); I and III are subcritical regions and II and IV supercritical ones. Note that a smooth invariant circle reappears near the thin part of the hourglass (region III) after its smoothness has been lost near the thick part (region II). This is in contradistinction to the dissipative standard-map case [7] in which there is no recurrence of invariant circles.

As the order Q of the tongue increases, the points J_i and J_i' move towards O_i, so that the critical line touches less of the curve (2.6). Furthermore, the whole line $K_iJ_iO_iJ_i'K_i'$ becomes flatter and the tongue width smaller. Therefore, following Bohr, Bak, and Jensen [7], within each tongue we choose the points O_i as the representative points, which will enable us to determine the critical line globally. The representative points for the high-order tongues just outside the $\frac{1}{3}$ tongue are denoted by circles in Figs. 3(a) and 3(b). They accumulate to the end points K_i and K_i' of the critical line within the $\frac{1}{3}$ tongue. Thus the critical line inside the tongue extends outside it. Globally, the critical line may be approximated by connecting the representative points in the neighboring tongues by straight-line segments. The approximation improves as one goes to the high-order tongues.

III. STRUCTURE OF THE CRITICAL LINE

Using the method discussed in the preceding section, we study the effects of the recurrence of invariant circles on the structure of the critical line by increasing the dissipation parameter from $b=0$.

Consider the case $z=0.1$. In the circle-map case $(b=0)$ the critical line is $k=1$, since the map is smooth and invertible for $k<1$, and it is noninvertible for $k>1$. Therefore there is no recurrence of invariant circles, although hourglass structures exist in the Arnol'd tongues with $Q>2$ (see Fig. 4). As shown in a previous paper [13], recurrence of an invariant circle depends not only on the structures of the nearby tongues, but also on their widths. In this case the widths of Arnol'd tongues are not large enough for recurrence of invariant circles. For $b=0.1$, the critical line is shown in Fig. 5(a). We have not observed any recurrence of invariant circles in all the cases studied, and thus the critical line seems to be

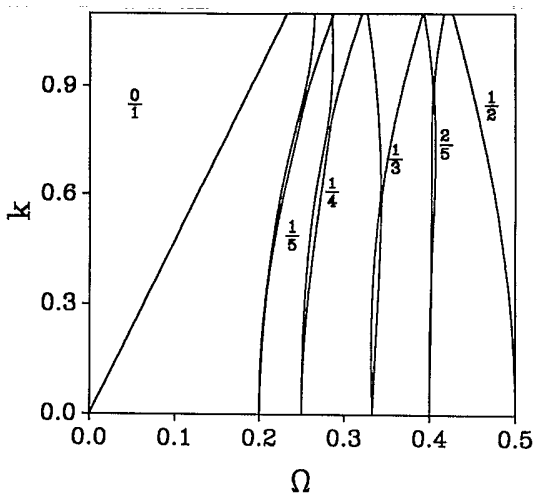

FIG. 4. Mode-locking diagram for $z=0.1$ and $b=0$.

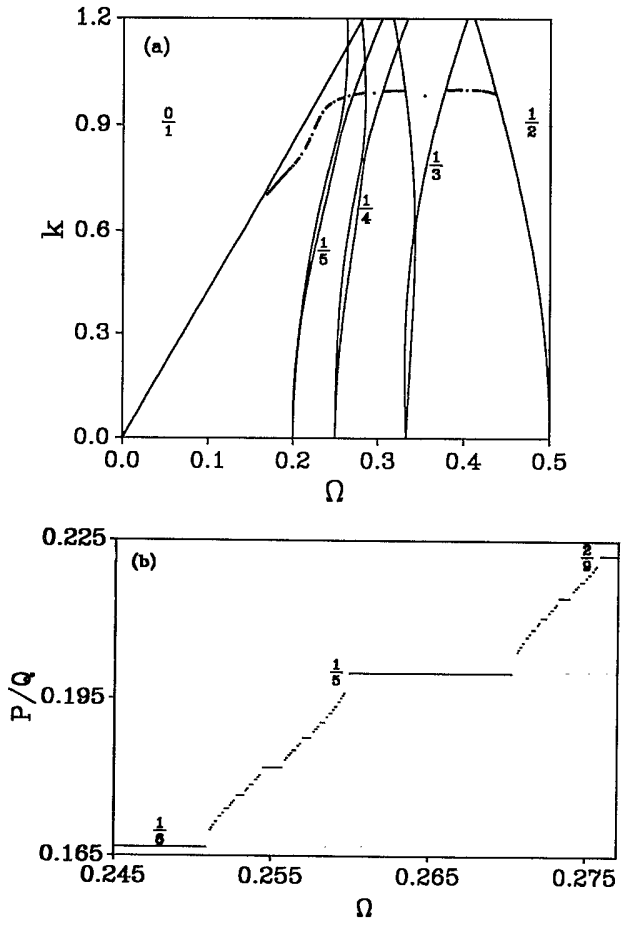

FIG. 5. (a) Critical line and (b) rotation number P/Q vs Ω at criticality for $z=0.1$ and $b=0.1$. In (a), the representative points of the tongues are plotted and a few low-order Arnol'd tongues are shown. Mode-locked steps larger than 2.1×10^{-5} are shown in (b).

smooth. However, since we have studied a finite number of invariant circles with relatively low periods, the possibility of recurrence of invariant circles with higher periods cannot be excluded. Within the finite resolution, the critical line seems to be a single-valued function of Ω, like the circle-map case. At this line the mode-locked intervals seem to trace up a devil's staircase [see Fig. 5(b)]. The mode-locked steps in the staircase were found by the method of Bohr, Bak, and Jensen [7], which will be explained later.

As b is increased, however, it has been observed that Arnol'd tongues become wider [e.g., compare Fig. 4 with Fig. 6(a)], so that smooth invariant circles reappear after their disappearance. Figure 6(a) shows the critical line for $b=0.3$. In Arnol'd tongue ($29/169 \leq \omega \leq 35/169$) near the $\frac{1}{5}$ Arnol'd tongue, smooth invariant circles reappear near the thin parts of the hourglass after they have disappeared near the thick parts, since Arnol'd tongues near the $\frac{1}{5}$ tongue become wide enough for recurrence of invariant circles. Like the case seen in Sec. II [see Figs. 3(a) and 3(b)], in each of the Arnol'd tongues in the recurrent region, there are three representative points [the bottom and top points of the "ellipse" (2.6) and the bottom point of the "hyperbola" (2.6)]. Due to the recurrence of smooth invariant circles, the critical line is folded back in the recurrent region near the $\frac{1}{5}$ tongue, and hence it becomes a multivalued function of Ω.

Unlike the preceding case ($b=0.1$), the mode-locked intervals on the folded part of the critical line trace a folded devil's staircase as shown in Fig. 6(b). The folded staircase is divided into five parts denoted by I, II, III, IV, and V in Fig. 6(b); in I, $\frac{1}{6} \leq \omega < \frac{1}{5}$, in both II and III, $\frac{1}{5} \leq \omega < \frac{35}{169}$, and in both IV and V, $\frac{29}{169} \leq \omega < \frac{1}{5}$. In parts I–III and V, Ω increases monotonically as the mode-locked intervals trace the folded staircase. However, it does not change monotonically in part IV [see Fig. 6(c)]; in part IV(a) ($\frac{20}{113} \leq \omega < \frac{1}{5}$), it decreases monotonically, while in part IV(b) ($\frac{29}{169} \leq \omega < \frac{20}{113}$), it increases monotonically.

The recurrent region expands as b is further increased, and hence the critical line becomes more folded back [compare Fig. 7 with Fig. 6(a)]. Let us see the expanding process in more detail. When $b=0.3$, there exists only a hyperbola-shaped curve (2.6) in the $\frac{1}{4}$ Arnol'd tongue whose representative point (i.e., the bottom point of the "hyperbola") is shown in Fig 6(a). As b is increased, a closed ellipse-shaped curve (2.6) appears and expands in the thick part of the hourglass. Thus, for $b=0.4$, the number of representative points in the $\frac{1}{4}$ tongue becomes three (see Fig. 7). However, there is still only one representative point [the bottom point of the "hyperbola"

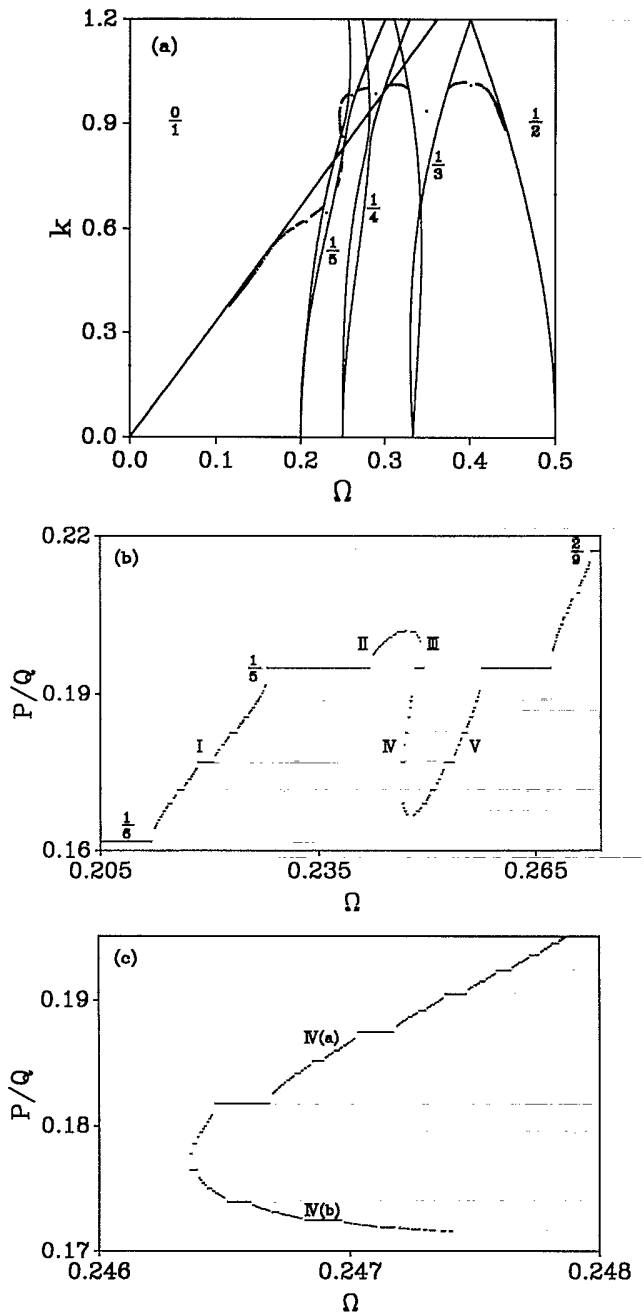

FIG. 6. Same as Fig. 4 except for $b=0.3$. Mode-locked steps larger than a given scale r, (b) $r=2.2\times10^{-5}$ and (c) $r=9.0\times10^{-7}$, are shown. Note that (c) is a magnification of part IV in (b).

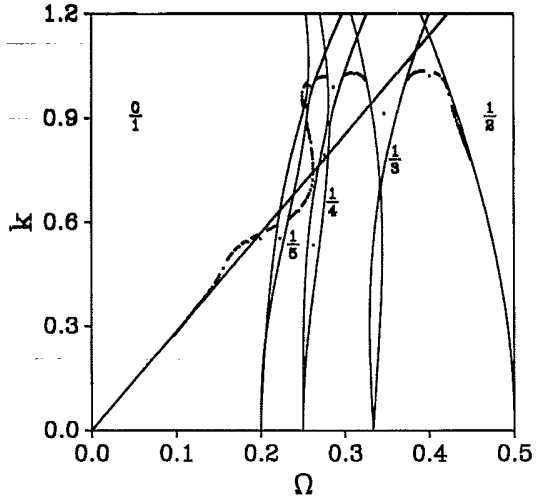

FIG. 7. Same as Fig. 4(a) except for $b=0.4$.

(2.6)] in each of the high-order tongues just outside the $\frac{1}{4}$ tongue. Therefore, unlike the case seen in Sec. II [see Fig. 3(a)], the curves on which crinkling up of the invariant circle takes place (crinkling curves) do not touch the tongue boundary near the thick part of the hourglass, which is shown in Fig. 8(a). Thus an isolated supercritical region exists inside the $\frac{1}{4}$ Arnol'd tongue.

As b is increased, the isolated supercritical region expands, and in each of the high-order tongues just outside the left tongue boundary, the number of representative points becomes three [see Fig. 8(b)]. Thus the crinkling curves intersect the left tongue boundary and connect with the critical line outside it. In this case, the crinkling curve on the right of the "ellipse" (2.6) does not yet touch the right tongue boundary. However, as b increases, this curve also intersects the right tongue boundary and connects with the critical line outside it (see Fig. 9). Thus the critical line becomes much more folded back as b increases [compare Figs. 6(a), 7, and 9].

Folding of the critical line is not the only effect of the

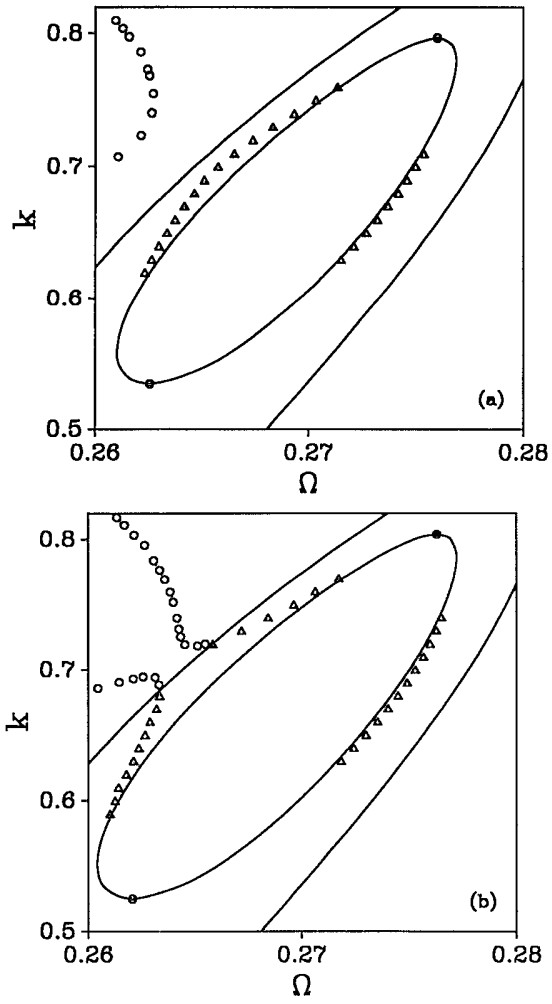

FIG. 8. Stability diagrams for the invariant circles near the thick part of the $\frac{1}{4}$ Arnol'd tongue (a) $z=0.1$, $b=0.4$ and for (b) $z=0.1$, $b=0.407$; symbols (○ and △) represent the same as those in Fig. 3. See text for other details.

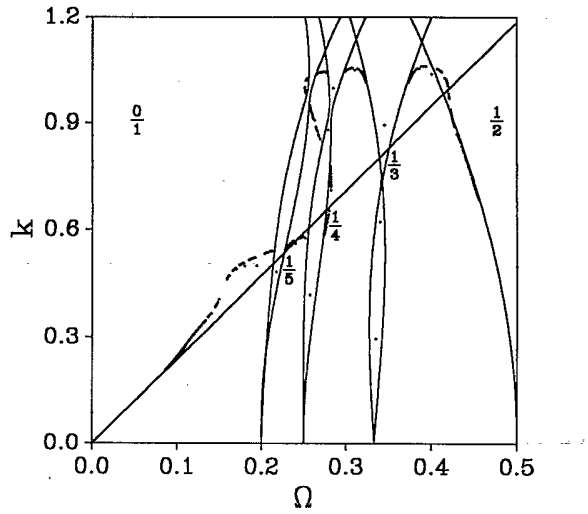

FIG. 9. Same as Fig. 4(a) except for $b=0.5$.

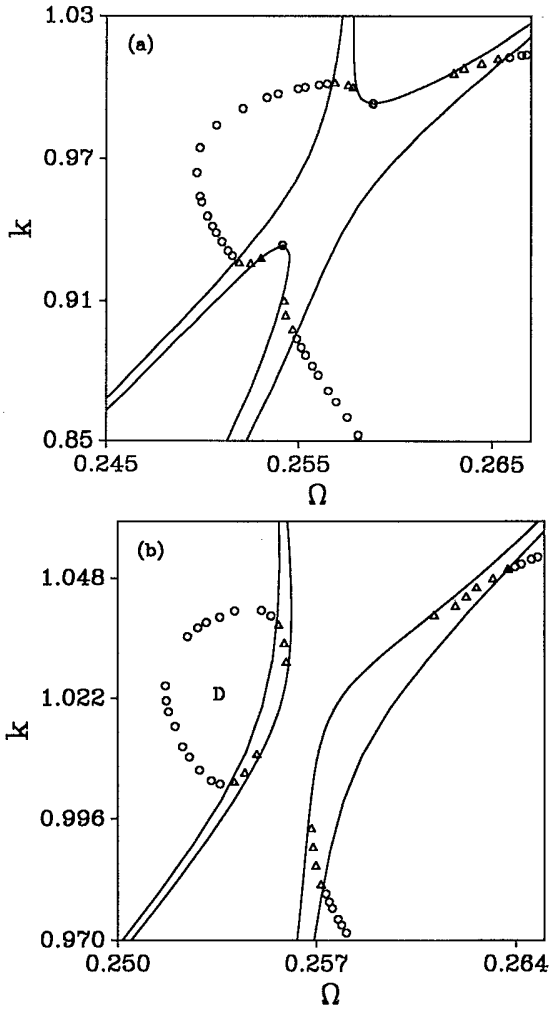

FIG. 10. Stability diagram for the invariant circles near the thin part of the $\frac{1}{5}$ Arnol'd tongue for (a) $z=0.1$, $b=0.4$ and (b) $z=0.1$ $b=0.55$; symbols (○ and △) denote the same as in Fig. 3. In (a), the lower curve inside the $\frac{1}{5}$ tongue is the upper part of the "ellipse" (2.6) and the upper curve the lower part of the "hyperbola" (2.6). In (b), there exists only one hourglass-shaped curve (2.6) inside the $\frac{1}{5}$ tongue. See text for other details.

recurrence of smooth invariant circles. As b increases, some part of the critical line becomes disconnected from the other part of it, as we shall see below. When $b=0.4$, there are three representative points in the $\frac{1}{5}$ Arnol'd tongue (see Fig. 7); the lowest (middle) point is the bottom (top) point of the ellipse-shaped curve (2.6) and the highest point the bottom point of the hyperbola-shaped curve (2.6). In this case, a subcritical region exists near the thin part of the hourglass [see Fig. 10(a)]. As b is increased the top point of the "ellipse" goes up towards the bottom point of the "hyperbola," and eventually the two points meet at a dissipation parameter value b^* ($b^*=0.498\,292\,86$). For $b>b^*$, the "ellipse" and the "hyperbola" merge into an open hourglass-shaped curve, and hence, two disconnected subcritical regions appear [see Fig. 10(b)]. In this case, there exists only one representative point which is the bottom point of the hourglass-shaped curve (e.g., see the $\frac{1}{5}$ Arnol'd tongue in Fig. 9). Thus a part of the whole critical line which encloses the left, isolated subcritical region denoted by D in Fig. 10(b) is disconnected from the other part of it. The mode-locked intervals on this disconnected part form an isolated part in the folded devil's staircase, which is shown in Fig. 11.

We have also studied the recurrence effects on the structure of the critical line for different values of z. Consider the case $b=0.3$. As the tuning parameter is decreased from $z=0.1$, the Arnol'd tongues become wider, so that the recurrent region expands. Therefore the critical line becomes more folded back [compare Fig. 12(a) with Fig. 6(a)]. However, as the tuning parameter increases from $z=0.1$, the Arnol'd tongues become narrower, and hence the recurrent region shrinks. Ultimately, the recurrent region seems to disappear [see Fig. 12(b)].

Finally, we study the metric properties of the irrational-rotation-number set (IRNS) on the critical line, using the method of Bohr, Bak, and Jensen [7]. To find the end points of the mode-locked steps, we approximate the critical line by connecting the representative points in the neighboring tongues by straight-line segments, as described in Sec. II. Then the endpoints of the P/Q steps are the intersections of the critical line with the boundaries of the P/Q Arnol'd tongues. For a given mode-locked step, the projection of the end points to the Ω axis determines the width of the step. The IRNS lies in the complement to the set of all mode-locked steps.

We have estimated the fractal dimension of the IRNS in a folded part of the critical line for $z=0.1$ and $b=0.3$ [see Fig. 6(a)]. The rotation number versus Ω is shown in Fig. 6(b). The mode-locked intervals trace a folded staircase, which is divided into six parts [see Figs. 6(b) and 6(c)].

In part I, we have found all the mode-locked steps with $Q\leq 161$ and calculated the total measure $M(r)$ of the complement (on the Ω axis) to the set of all mode-locked steps which are larger than a given scale r. Then,

$$N(r)=M(r)/r$$

approximates the number of r intervals needed to cover the IRNS. As r goes to zero,

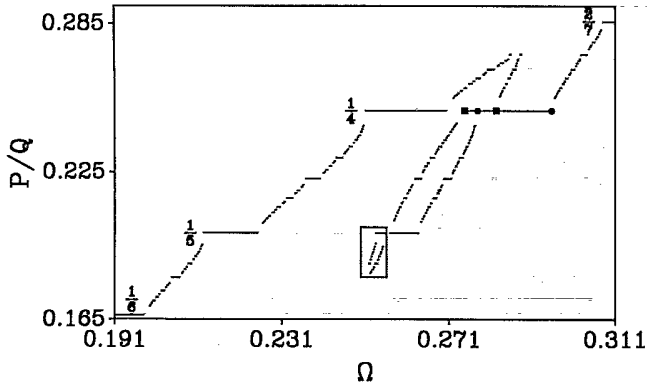

FIG. 11. Rotation number P/Q vs Ω at criticality for $z=0.1$ and $b=0.55$. Mode-locked steps larger than 5.7×10^{-5} are shown. For $\omega=\frac{1}{5}$, the second and third steps overlap due to the *multivaluedness* of the critical line; their end points are denoted by squares and circles, respectively. Note that the part inside the box ($\frac{9}{49}\leq\omega\leq\frac{1}{5}$) is isolated from the other part.

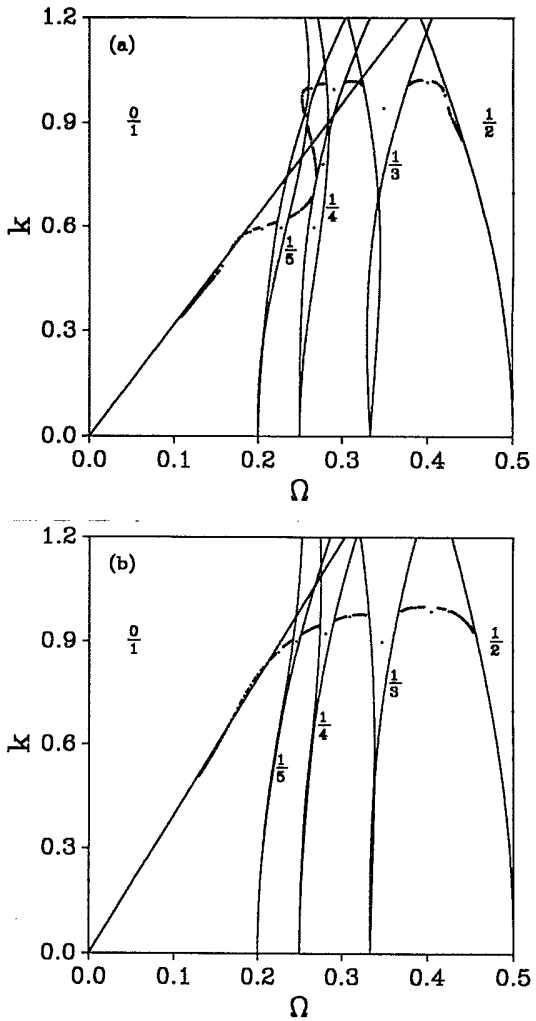

FIG. 12. Critical lines for (a) $z=0.05$, $b=0.3$ and (b) $z=1.0$, $b=0.3$.

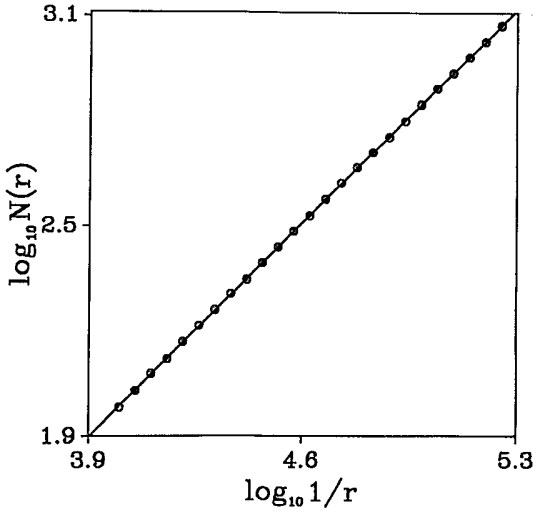

FIG. 13. Plot of $\log_{10}N(r)$ vs $\log_{10}1/r$ at criticality for $z=0.1$ and $b=0.3$.

$$N(r)\sim r^{-D} .$$

The exponent D is the fractal dimension of the IRNS. In Fig. 13, $\log_{10}N(r)$ has been plotted versus $\log_{10}1/r$ for 25 values of r in the interval $(1.0\times10^{-4},5.0\times10^{-6})$. The data points are fit well by a straight line with slope

$$D=0.871\pm0.004 .$$

The estimated value of D agrees well with that obtained in the sine-circle map [6]. We have also obtained the estimates of D in the other parts. Within numerical accuracy, those values of D are the same as that obtained in part I. Therefore the scaling behavior coincides with that found in the sine-circle map.

IV. SUMMARY

We have studied the recurrence effects on the structure of the critical line in the dissipative Wilbrink map with small z values. In the circle-map case ($b=0$) the critical line is $k=1$. Hence there is no recurrence of invariant circles, although hourglass structures exist in the Arnol'd tongues with $Q>2$. Recurrence of invariant circles depends not only on the structures of Arnol'd tongues, but also on their widths [13]. In this case the widths of Arnol'd tongues are not large enough for recurrence of invariant circles. For small b we have not observed any recurrence of invariant circles in all the cases studied, and thus the critical line seems to be smooth, like the circle-map case. However, since we have studied a finite number of invariant circles with relatively low periods, the possibility of recurrence of invariant circles with higher periods cannot be excluded. Due to the finite resolution, unfortunately we were unable to estimate a critical value of b, below which there is no recurrence of invariant circles, and above which the map exhibits recurrence effects. However, as b is further increased, it has been observed that Arnol'd tongues become wider, so that smooth invariant circles reappear near the thin parts of the hourglass after they have disappeared near the thick parts. Due to the recurrence effects, the critical line becomes folded back and has disconnected parts. Therefore, at this line, the mode-locked intervals trace a folded devil's staircase with isolated parts. In spite of the complicated structure of the critical line, the critical scaling of the irrational-rotation-number set on the line is the same as that found in the sine-circle map.

ACKNOWLEDGMENTS

We would like to thank Dr. H. Kook and Dr. S. Y. Lee for useful discussions. This work was supported by the Non-Directed Research Fund, Korea Research Foundation.

[1] H. Curry and J. A. Yorke, in *The Structure of Attractors in Dynamical Systems*, edited by N. Markley, J. Martin, and W. Perrizo, Lecture Notes in Mathematics Vol. 668 (Springer, Berlin, 1977), p. 48.
[2] D. G. Aronson, M. A. Chory, G. R. Hall, and R. P. McGehee, Commun. Math. Phys. **83**, 303 (1982).
[3] S. J. Shenker, Physica D **5**, 405 (1982).
[4] M. J. Feigenbaum, L. P. Kadanoff, and S. J. Shenker, Physica D **5**, 370 (1982).
[5] S. Ostlund, D. Rand, J. Sethna, and E. Sigga, Physica D **8**, 303 (1983).
[6] M. H. Jensen, P. Bak, and T. Bohr, Phys. Rev. A **30**, 1960 (1984).
[7] T. Bohr, P. Bak, and M. H. Jensen, Phys. Rev. A **30**, 1970 (1984).
[8] P. Alstrøm, Commun. Math. Phys. **104**, 581 (1986).
[9] W. M. Yang and B. L. Hao, Commun. Theor. Phys. **8**, 1 (1987).
[10] P. Alstrøm, M. T. Levinsen, and D. R. Rasmussen, Physica D **26**, 336 (1987).
[11] X. Wang, R. Mainieri, and J. H. Lowenstein, Phys Rev. A **40**, 5382 (1989).
[12] B. Hu, A. Valinia, and O. Piro, Phys. Lett. A **144**, 7 (1990).
[13] S. Y. Kim and B. Hu, Phys. Rev. A **44**, 934 (1991).
[14] B. V. Chirikov, Phys. Rep. **52**, 263 (1979).
[15] J. M. Greene, J. Math. Phys. **20**, 1183 (1979).
[16] J. Wilbrink, Physica D **26**, 358 (1987).
[17] H. J. Schelnhuber and H. Urbscht, Phys. Rev. Lett. **54**, 588 (1985).
[18] F. Axel and S. Aubry, J. Phys. A **20**, 4873 (1987).
[19] J. Ketoja and R. S. MacKay, Physica D **35**, 318 (1989).
[20] R. B. Griffiths and W. Chou, Phys. Rev. Lett. **56**, 1929 (1986).
[21] V. I. Arnold, Trans. Am. Math. Soc., Second Ser. **46**, 213 (1965); M. R. Herman, in *Geometry and Topology*, edited by J. Palis and M. do Carmo, Lecture Notes in Mathematics Vol. 597 (Springer, Berlin, 1977), p. 271.